AGU PUBLICATIONS

Geophysical Research Letters

RESEARCH LETTER
10.1002/2017GL073891

Key Points:
- All 27 simulations produced large-scale eastward propagating signals in precipitation (the MJO) but with different occurrence frequencies
- There is no statistically significant distinction in the strength and propagation speeds of MJO events simulated by most of these models
- It is hypothesized that a model can produce the MJO only in a particular background state

Correspondence to:
J. Ling,
lingjian@lasg.iap.ac.cn

Citation:
Ling, J., C. Zhang, S. Wang, and C. Li (2017), A new interpretation of the ability of global models to simulate the MJO, *Geophys. Res. Lett.*, *44*, 5798–5806, doi:10.1002/2017GL073891.

Received 19 APR 2017
Accepted 11 MAY 2017
Accepted article online 15 MAY 2017
Published online 12 JUN 2017

A new interpretation of the ability of global models to simulate the MJO

Jian Ling[1,2], Chidong Zhang[3], Shuguang Wang[4], and Chongyin Li[1]

[1]State Key Laboratory of Numerical Modeling for Atmospheric Sciences and Geophysical Fluid Dynamics, Institute of Atmospheric Physics, Chinese Academy of Sciences, Beijing, China, [2]University of Chinese Academy of Sciences, Chinese Academy of Sciences, Beijing, China, [3]NOAA Pacific Marine Environmental Laboratory, Seattle, Washington, [4]Department of Applied Physics and Applied Mathematics, Columbia University, New York, New York, USA

Abstract Statistical diagnostics have led to a common perception that only few global models can reproduce the Madden-Julian Oscillation (MJO). Here we demonstrate, using a method of tracking individual MJO events, that this perception is incorrect. Of 27 global model simulations diagnosed, all produced large-scale slowly eastward propagating signals in precipitation, which are taken as manifestations of the MJO. The difference is some model produced them frequently, others infrequently. There is no statistically significant distinction between the strength and propagation speeds of MJO events produced by most of these models. A hypothesis is proposed to interpret our results: A model can produce the MJO only in a particular background state. If the background state of a model can be constantly in a condition that is conducive to its production of the MJO, this model simulates the MJO frequently. If not, this model can still produce the MJO but only infrequently when its seasonal background state occasionally migrates into a condition that is conducive to its production of the MJO. Preliminary results from testing this hypothesis are presented.

1. Introduction

Since the Madden-Julian Oscillation (MJO) was first documented [*Madden and Julian*, 1971, 1972], its simulation by global models has always been a daunting challenge [*Hayashi and Golder*, 1986; *Lau and Lau*, 1986; *Slingo et al.*, 1996; *Sperber et al.*, 1997; *Waliser et al.*, 2003; *Lin, et al.*, 2006; *Zhang et al.*, 2006; *Kim et al.*, 2009; *Hung et al.*, 2013; *Jiang et al.*, 2015]. While progress has been slowly made in this regard [*Lau and Waliser*, 2011; *Zhang*, 2013; *Ling et al.*, 2017], it is widely perceived that most current global models still cannot produce the MJO. This perception is based on model diagnostics using methods of extracting statistical signals of the MJO. These methods include time-space spectrum analysis and time-lag correlation of precipitation or other variables immanent to the MJO [*Lin, et al.*, 2006; *Kim et al.*, 2009; *Waliser et al.*, 2009; *Hung et al.*, 2013, *Jiang et al.*, 2015]. In most model simulations, there is no dominant statistical eastward propagating signal: The ratio of MJO power to its westward propagating counterpart of the same frequencies and zonal wave numbers is equal or less than one [e.g., *Lin, et al.*, 2006, Figure 10; *Hung et al.*, 2013, Figure 8], and time-lag regression shows stationary or even westward propagating patterns [e.g., *Jiang et al.*, 2015, Figures 3 and 4].

These results have prompted many to wonder why so few global models can produce the MJO. A common belief is that a model's ability of simulating the MJO depends on specific features of its cumulus parameterization scheme, such as its entrainment/detrainment rate [*Bechtold et al.*, 2008; *Fu and Wang*, 2009; *Hannah and Maloney*, 2014], closure assumption [*Zhang and Mu*, 2005; *Mu and Zhang*, 2008; *Benedict et al.*, 2013, *Peters et al.*, 2017], or convective momentum transport [*Wu et al.*, 2007; *Ling et al.*, 2009; *Miyakawa et al.*, 2012]. Efforts have been made to design process-oriented diagnostic metrics that may help identify properties in parameterization schemes, especially cumulus schemes, which may be essential to MJO simulations [*Hannah and Maloney*, 2011; *Hirons et al.*, 2013; *Zhou et al.*, 2012; *Kim et al.*, 2014, *Ahn et al.*, 2017; *Peters et al.*, 2017].

Studies on MJO simulations to date mostly emphasize on statistical signals (e.g., spectral power and regression patterns) of the MJO in multiyear simulations. Lost in such emphases are characteristics of individual MJO events in model simulations. Such characteristics include starting and ending longitudes, strength, propagation speeds, longitudinal ranges, life spans, and intervals between adjacent MJO events. Information of these characteristics of individual MJO events may provide new insights to the issues of MJO simulations.

Motivated by this, we in this study reevaluated MJO signals in 27 simulations by global models that were diagnosed by *Jiang et al.* [2015]. Instead of only examining statistical signals of the MJO in these simulations, we applied an MJO tracking method [*Ling et al.*, 2014; *Zhang and Ling*, 2017] to identify individual MJO events in the simulations as well as observations. We introduce the data and method in section 2, present the results in section 3, and discuss their implications in section 4.

2. Data and Method

2.1. Data

Daily precipitation (0.25° × 0.25°, 1998–2015) from Tropical Rainfall Measuring Mission (TRMM) 3B42v7 Multisatellite Precipitation Analysis [*Huffman et al.*, 2007] was used to identify individual MJO events and mean precipitation pattern in observations. Zonal wind and specific humidity (0.75° × 0.75°,1998–2015) from the European Centre for Medium-Range Weather Forecasts Interim Reanalysis (ERA-I) [*Dee et al.*, 2011] were used as surrogates of observations in calculating background states of the atmosphere to compare with those in model simulations.

Twenty-year global model simulations from the Global Multi-Model Evaluation Project on Vertical Structure and Diabatic Processes of the MJO (GASS-YoTC-MJO) [*Petch et al.*, 2011] were assessed for their ability of producing the MJO. The project includes 27 simulations by 20 atmospheric-only global models, six fully atmosphere-ocean coupled models, and one partially coupled model. Their full descriptions are available in *Jiang et al.* [2015].

2.2. MJO Tracking Method

The MJO tracking method used in this study was first introduced by *Ling et al.* [2014] and recently updated by *Zhang and Ling* [2017]. The basic idea is to track the eastward propagation of positive precipitation anomalies along the equator and identify MJO events based on known observed characteristics of the MJO, such as its propagation speed and intraseasonal timescales. Applying this tracking method requires several parameters (e.g., reference longitude, tracking domain, range of propagation speed, minimum interval, and propagation distance of the MJO) to be initially selected based on one's perception of the MJO. Once these parameters are selected, MJO events are identified without further human intervention, hence objectively and reproducibly. The tracking method provides other properties of the selected MJO events (e.g., starting and ending longitudes, propagation ranges in longitude, strength in terms of precipitation, and life spans). All these characteristics are not available from MJO indices based on empirical orthogonal functions [*Wheeler and Hendon*, 2004; *Kiladis et al.*, 2014; *Lafleur et al.*, 2015; *Liu et al.*, 2016]. These tracked characteristics are not sensitive to slight changes in the selected parameters. A full description of this method can be found in *Zhang and Ling* [2017].

This MJO tracking method was applied to intraseasonally filtered daily precipitation anomalies in the equatorial region from both observations and model simulations using the same parameters as in *Zhang and Ling* [2017]. Daily anomalies in precipitation were generated by removing the daily climatology (omitting 29 February in leap years). They were then averaged over a latitudinal belt of 15°S–15°N. A time-space fast Fourier transform was used to obtain the large-scale (zonal wave numbers 1–10) and intraseasonal (20–100 days) signals. The filtering retains both eastward and westward propagating signals in this study. The common practice of retaining only eastward propagating signals is appropriate for observations [*Gottschalck et al.*, 2013; *Zhang and Ling*, 2017] in which eastward signals clearly dominate the intraseasonal band [*Zhang and Hendon*, 1997], but it is inappropriate for model simulations where westward propagating signals can be as strong as or even stronger than eastward signals in the intraseasonal band [*Zhang et al.*, 2006; *Jiang et al.*, 2015]. For consistency, daily precipitation from TRMM (0.25° × 0.25°) was interpolated to the same spatial grids (2.5° × 2.5°) of the model simulations prior to the filtering.

2.3. Pattern Correlation

Pattern correlation between time-lag regression for precipitation anomalies from model simulations and observations was used by *Jiang et al.* [2015] to objectively and quantitatively measure model capability of simulating the MJO. This method was adapted in this present study with a modification. In *Jiang et al.* [2015], two pattern correlation coefficients, each with a reference point over the Indian Ocean and Pacific Oceans, respectively, were averaged. In this present study, only the pattern correlation with a reference point at 90°E was used to emphasize MJO signals over the Indian Ocean. The reason for this is that in observations

most MJO events form over the Indian Ocean, and only ~50% of them propagate through the Indo-Pacific Maritime Continent and reach the western Pacific [*Zhang and Ling*, 2017]. Our modification yields almost consistent ranking of model capability of producing the MJO as in *Jiang et al.* [2015]. It should be pointed out that including the reference point(s) in the pattern correlation calculation inflates the correlation coefficient. For example, when a model does not show clear eastward propagation in its time-lag regression map, its pattern correlation with observations can still be greater than 0.5 and significant at the 95% confidence level [*Jiang et al.*, 2015]. This inflation in the pattern correlation coefficient, however, affects negligibly the ranking of the model capability of simulating the MJO.

3. Results

The capability of simulating the MJO by the 27 models was ranked using the measure of pattern correlation briefly described in section 2.3. Based on this ranking, they were grouped into three tiers of nine simulations in each, as illustrated in Figure 1a: the top (blue), middle (green), and bottom (orange) tiers, with their scores above, near, and below the total average, respectively. Models in the top tier produced evident eastward propagating signals in their time-lag regression map (contours in Figure 2b) similar to the TRMM observations (contours in Figure 2a). In contrast, models in the bottom tier do not show obvious eastward propagating signal in their time-lag regression map (contours in Figure 2c). They are models incapable of producing the MJO in a statistical sense.

When the MJO tracking method was applied to these model simulations, we found that all models, including those in the bottom tier, produced MJO events. As an example, a model (CFS2) from the bottom tier that shows only westward propagation signals in its time-lag correlation map [*Jiang et al.*, 2015, Figure 3] produced an MJO event (Figure 2e) that has a comparable amplitude to an MJO event produced by a model (PNU_CFS) from the top tier (Figure 2d). The composite of all tracked MJO events from models in the bottom tier shows systematic eastward propagation in precipitation anomalies (colors in Figure 2c). This is expected but in a sharp contrast to their averaged lag-regression (contours), which gives an impression that these models cannot produce the MJO at all. In these models, the MJO signals are, however, much weaker over the Pacific than Indian Ocean compared to the observations (Figure 2a) and models in the top tier (Figure 2b). This is perhaps an illustration of the exaggerated barrier effect of the Maritime Continent in models [*Inness and Slingo*, 2006; *Kim et al.*, 2009; *Seo et al.*, 2009].

Based on our diagnostics using the MJO tracking method, the difference between the models is not whether they can produce the MJO; it is how often they do. This difference is illustrated in Figure 1b, where longitudinal distributions in occurrence frequencies of MJO initiation derived from the tracking method are plotted for the observations and model simulations. All models suffer from a major bias in their MJO simulations: In the observation, most MJO events form over the Indian Ocean, whereas simulated MJO initiation is more evenly distributed in longitude over the Indo-Pacific region. Compared to the observations, almost all models underestimate the MJO occurrence frequency, particularly during boreal summer. Results presented in the rest of this study are for the extended boreal winter (October–March) and for only the tracked MJO events that form over the Indian Ocean or to its west (their tracks passing through 90°E) in both observations and simulations.

Most of the models severely underestimate the occurrence frequency of MJO events formed west of 90°E, with their averaged occurrence frequency only less than a half of the observed (Figure 3a). The major difference between models in the top and bottom tiers ranked by the pattern correlation is their occurrence frequencies of the simulated MJO. MJO simulation scores based on the pattern correlation are significantly (at the 95% confidence level) correlated to the occurrence frequency of MJO events. This is easy to understand: No matter how well a model may produce the MJO, its pattern correlation based on the time-lag regression must be relatively low if it produces only a few MJO events in its 20 year simulations.

Models in the bottom tier, which cannot produce statistics of the MJO (Figure 2c), can produce MJO events of many similar qualities as models in the top tier. Based on Kolmogorov-Smirnov (KS) tests, propagation ranges of simulated MJO events by the top-tier models are significantly (at 95% confidence level) longer than those simulated by the bottom-tier models (Figure 3b), but their strength (Figure 3c) and speeds (Figure 3d) are not distinguishable between the top and bottom tiers. The more commonly used MJO scores based on the

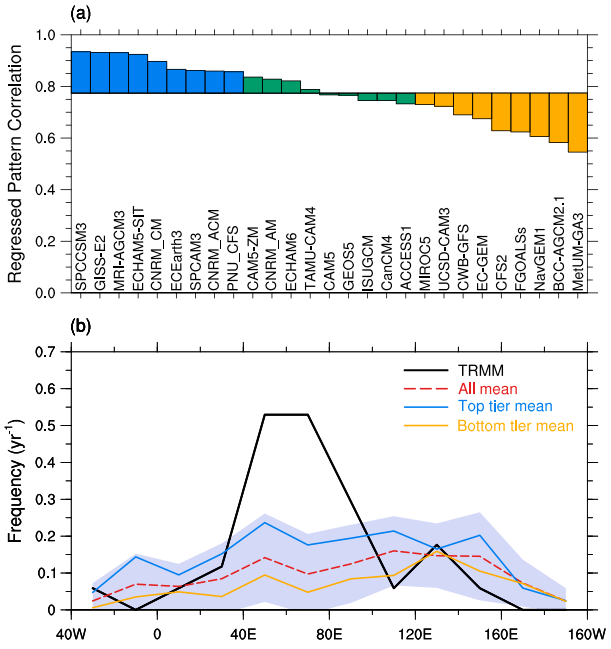

Figure 1. (a) Skill scores of MJO simulations based on pattern correlations of regressed precipitation anomalies from models and the TRMM observations. The horizontal line marks their average. The three colors mark the top, middle, and bottom tiers with their score above (blue), near (green), and below (orange) the average, respectively. (b) Longitudinal distributions of MJO initiation frequencies (yr^{-1}) in the TRMM observations (black solid line), all model average (red dashed line), nine top-tier models average (blue solid line), and nine bottom-tier model average (orange). The light blue shade marks the one standard deviation for all models. The longitudinal bin width is 20°. The pattern correlations between the models and observations were calculated over 60°E–180° and day −20 to day 20 (see Figure 2).

pattern correlation measure occurrence frequencies and the propagation ranges, but not other properties of the simulated MJO, and certainly not whether a model can produce the MJO.

There might be a concern that if a model cannot produce the observed occurrence frequency of eastward propagating large-scale signals in precipitation, whether these signals can be considered as simulated MJO events at all. They probably should not, if the MJO is viewed as an oscillatory phenomenon that occurs frequently and regularly. In observations, however, it does not. There are plenty of examples of isolated MJO events without any one immediately before and after. There are also examples of long periods (e.g., 3–4 months) without a single MJO event. The MJO can therefore be viewed as individual pulses [*Salby and Hendon*, 1994; *Yano et al.*, 2004] that may be connected to others as in successive MJO events [*Matthews*, 2008] and may not. It is based on this pulse viewpoint of the MJO that we suggest occurrence frequency of eastward propagating large-scale anomalies in precipitation is not a necessary feature for judging whether a model can simulate individual MJO events.

Based on these results, we suggest that in addition to statistical signals, we need to evaluate MJO simulations in terms of the characteristics of individual MJO events. We also argue that the right question to ask regarding model capability of simulating the MJO is not why some models can produce the MJO and others cannot. They all produce individual MJO events to a certain degree. The right question should be why some models produce MJO events more frequently than others.

We propose a hypothesis to address the latter question: A model can produce the MJO but only in a certain background state, regardless whether it is similar to the observed. In this hypothesis, the background state of a model can be constantly in a condition that is conducive to its production of the MJO. This model simulates the MJO frequently. In another model, its background state can be constantly in a condition unfavorable to its production of the MJO. Its background state, however, may change slowly and occasionally migrate into a condition that is conducive to its MJO production. This model produces the MJO infrequently. Based on this hypothesis, it is possible that a model produces the MJO even if its background state that is conducive to its MJO production is very different from the observed.

According to this hypothesis, the background state in which a model produces the MJO should be different from that in which the same model does not produces the MJO. One way to evaluate this hypothesis is to examine whether the difference in these two background states is statistically significant. There is, however, no consensus as what fields constitute the background state particularly for the MJO. Variables commonly used to construct background states in MJO studies include precipitation, low-level zonal wind, and low-level humidity [*Slingo et al.*, 1996; *Hendon et al.*, 2000; *Kemball-Cook et al.*, 2002; *Inness et al.*, 2003; *Zhang et al.*, 2006].

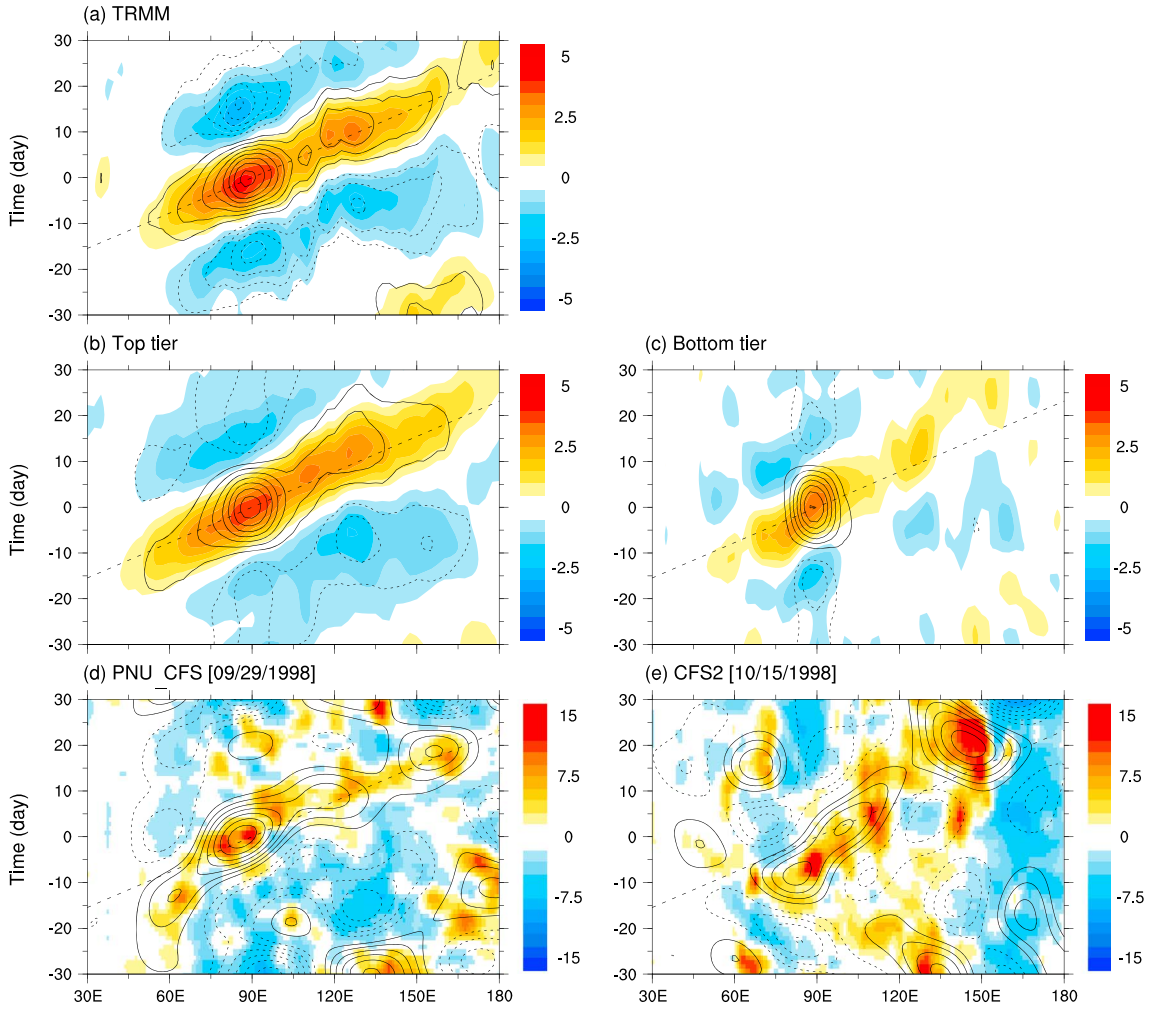

Figure 2. Time-longitude (15°S–15°N) diagrams of regressions (contours, interval 0.25) and composites (colors) of tracked MJO precipitation (mm d^{-1}) during October–March for (a) TRMM, (b) simulations in the top tier, and (c) simulations in the bottom tier. Time-longitude (15°S–15°N) diagrams of precipitation anomalies (colors, mm d^{-1}) and their 5 day running mean (contours, interval 1) from (d) the PNU_CFS simulation (time 0 on 29 September 1998) and (e) the CFS2 simulation (time 0 on 15 October 1998). Time 0 is when an MJO track crosses 90°E. The dashed contours are for negative values, and the zero contours omitted. The dashed straight lines mark the 5 m s^{-1} eastward propagation speed. Regressions in Figures 2b and 2c were calculated for each individual simulation and then averaged over the top and bottom tiers, respectively.

We used seasonal means of precipitation, zonal wind at the 850 hPa level, and weighted average of specific humidity between 925 and 700 hPa to define background states. Here a season is an extended boreal winter (October–March). For a given model simulation, a season was treated as one with the MJO if during which any MJO event was detected by the tracking method; otherwise, it was taken as a season without the MJO. The background states are measured by pattern correlation, root-mean-square error (RMSE), and mean bias (difference in domain-averaged seasonal means) calculated against long-term seasonal mean of TRMM precipitation and ERA-I wind and humidity over a domain of 60°E–180° and 15°S–15°N where the observed MJO prevails. Differences between the background states for seasons with and without the MJO are evaluated by comparing the probability density distributions of the three measures. A KS test was used to assess whether their differences are significant at the confidence level of 95% ($p < 0.05$).

Ideally, the two background states should be compared for each individual model. But with the 20 year simulations we have, this would suffer from insufficient sampling for robust statistics. We decided to compare seasons with and without the MJO for all simulations combined. This faces a problem: Even if our hypothesis is correct, the background states for all-model seasons with and without the MJO may not be significantly different if there is no systematic relationship between background states in the simulations and observations. The results turn out not to be the case.

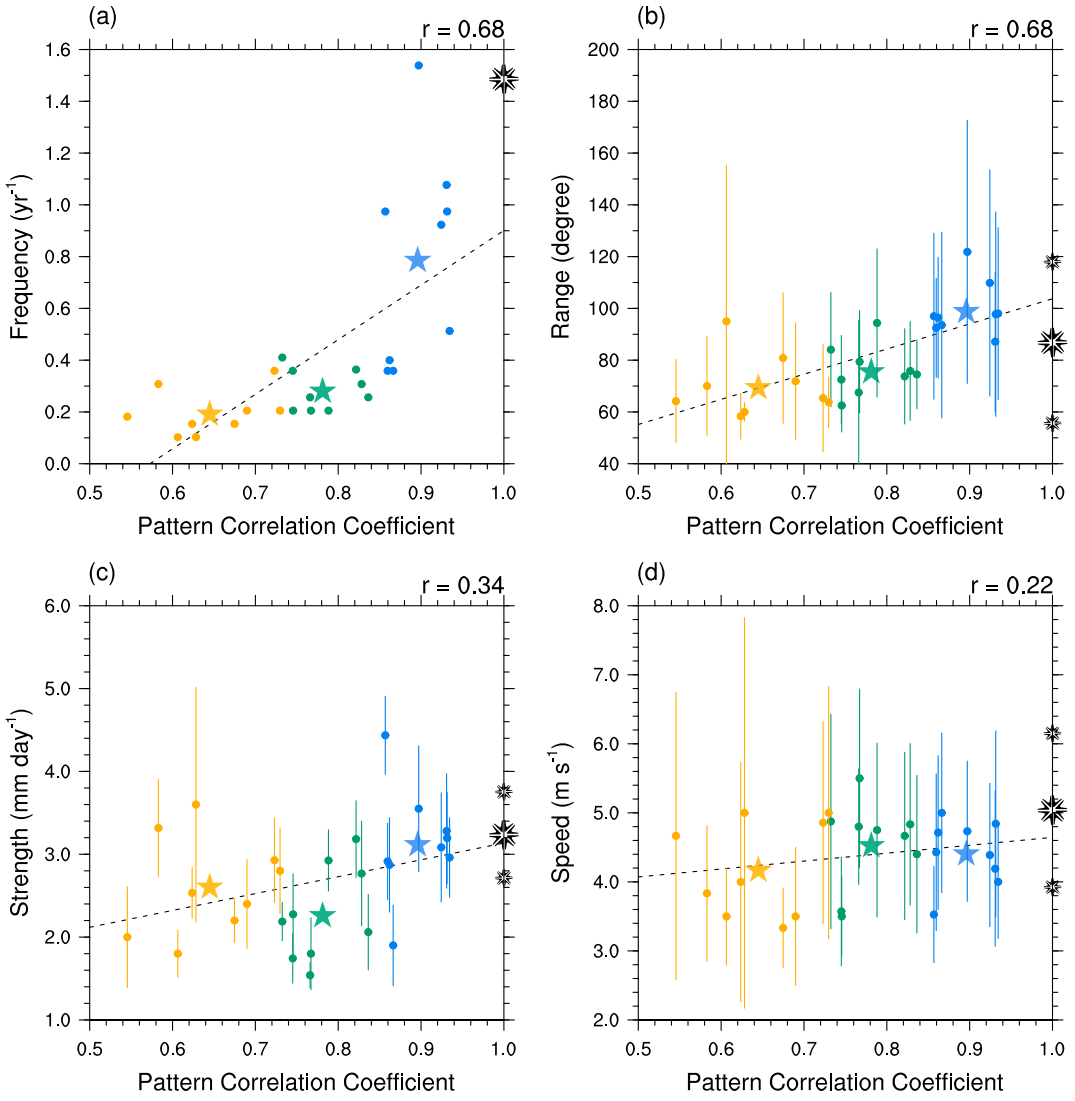

Figure 3. Scatter diagrams of MJO simulation skill scores in terms of pattern correlation versus averaged (a) occurrence frequencies (yr^{-1}), (b) propagation ranges (longitude), (c) strength (averaged rain rate in mm d^{-1}), and (d) speeds (m s^{-1}) of tracked MJO events in the model simulations. Their correlation coefficients are given on the top right corners. The blue, green, and orange dots represent models of the top, middle, and bottom tiers, respectively, as defined in Figure 1a, and the corresponding stars represent their means. The vertical whiskers mark one standard deviations. The black dotted lines denote linear fit by least squares means. The large and small octagonal stars on the right ordinates mark observed means and one standard deviations. The pattern correlation between the models and TRMM was calculated for 60°E–180° and −20–20 days (see Figure 2).

Model background states defined by the three variables are all significantly different between seasons with and without the MJO in the simulations in terms of their pattern correlation with the observations (Figures 4a–4c). Pattern correlation is in general higher for seasons with the MJO than those without. It suggests that overall, a background state with its spatial pattern closer to the observed is more likely to be conducive to MJO production. But it should be noticed that such a background state does not guarantee a production of the MJO and the MJO can be produced in a background state with its spatial pattern very different from the observed (low pattern correlation). Among the three variables used to define the background state, zonal wind at 850 hPa appears to be the most influential to MJO simulations. It is significantly different between seasons with and without the MJO in the simulations in terms of all three measures (Figures 4b, 4e, and 4h). RMSE of the low-level zonal wind is in general smaller for seasons with the MJO than those without. Its mean bias is, however, slightly higher for seasons with the MJO than those

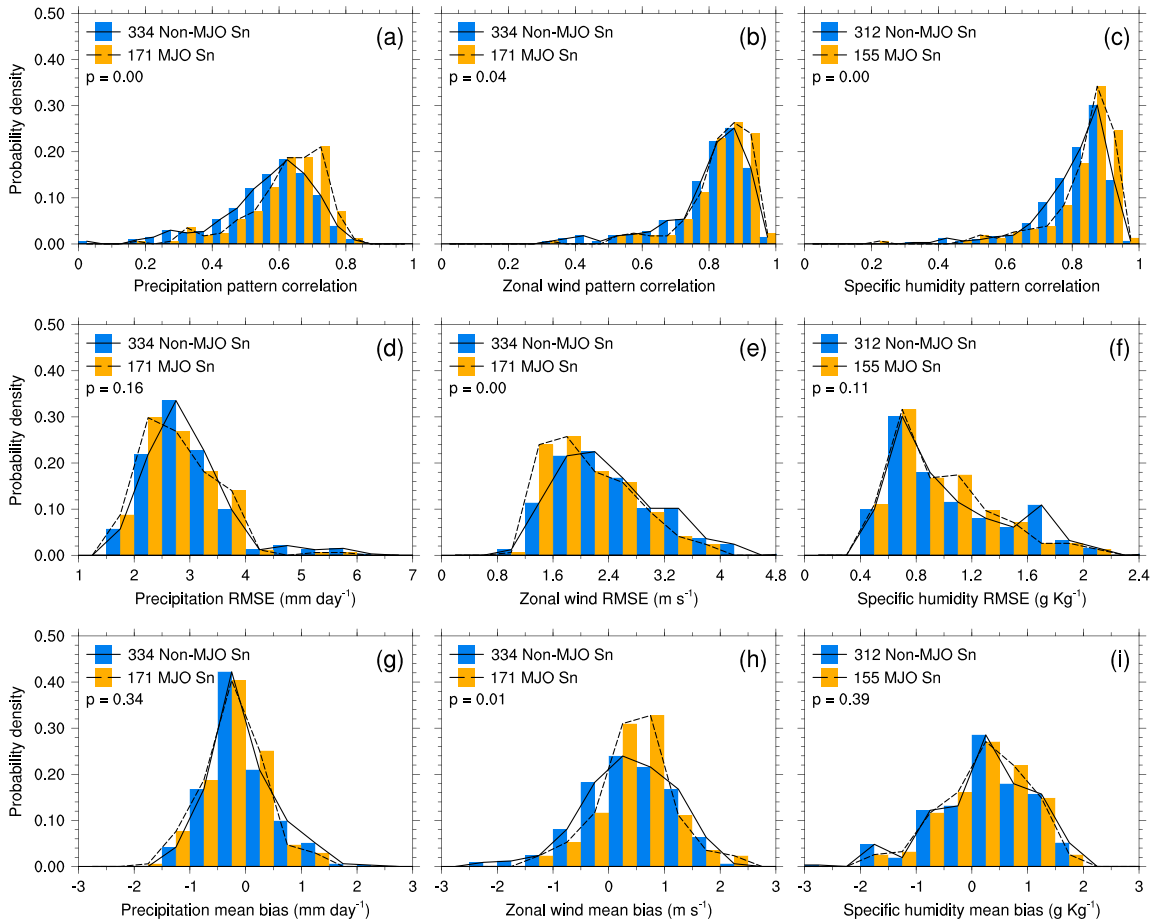

Figure 4. Probability density distributions of background states with the MJO (orange bars and dashed curves) and without (blue bars and solid curves) for the model simulations. Background states are defined using October–March means of (a, d, and g) precipitation, (b, e, and h) zonal wind at 850 hPa, and (c, f, and i) weighted-average specific humidity between 925 and 700 hPa and are measured by their (a–c) pattern correlation, (d–f) root-mean-square error (RMSE), and (g–i) mean bias with respective to observed climatology in a domain of 60°E–180° and 15°S–15°N. Total MJO and non-MJO seasons used and *p* values of KS tests are given in each panel. Specific humidity is not available from two simulations, hence different total seasons.

without. This implies that a westerly bias may compensate other biases and errors in models to give a more favorite condition for MJO production than an easterly bias [*Inness et al.*, 2003]. Nevertheless, as seen in pattern correlation, small RMSE and mean bias in the low-level zonal wind do not guarantee an MJO production.

4. Discussion

The results from this study indicate that the enigma of global model simulations of the MJO is not why some models can and others cannot produce the MJO. It is not even why some models produce strong and others weak MJO events. It is why some models produce the MJO frequently and other infrequently. We hypothesized that the central piece of this puzzle is the background state. The importance of the background state has been proposed by many to explain differences in MJO statistics simulated by different models [*Slingo et al.*, 1996; *Hendon et al.*, 2000; *Kemball-Cook et al.*, 2002; *Inness et al.*, 2003; *Zhang et al.*, 2006]. Here we extend it to explain how occurrence frequency of simulated MJO, which is the main reason for simulated MJO statistics, depends on seasonal background states that may vary from year to year within a given model.

Our results may also explain the conundrum wherein a model may produce statistical signals of the MJO in its climate simulation but its MJO prediction skill using observed initial conditions is very low, or it may predict the MJO well but cannot produce MJO statistics in a climate simulation [*Klingaman et al.*, 2015]. It all depends

on the background state that allows it to produce the MJO. If that background state is close to the observed, this model may predict the MJO well starting from an observed initiation condition until its background state drifts away as the lead time increases. But this model may not be able to simulate MJO statistics if the seasonal background state in its climate simulation is very different from the observed most of time. If the background state conducive to MJO production by a model is very different from observations, this model may produce MJO statistics in its climate simulation, but it may not predict the MJO well with observed initial conditions.

Our hypothesis is in line with the previous notion that the background state is a key factor for MJO simulations. But in our hypothesis, a model background state very different from observations would not necessarily prevent the MJO from being produced by the model. If our hypothesis is correct, it sets a high bar for MJO simulations, which demands a higher-level scrutiny of models used as tools to understand MJO physics. If these models cannot produce a background state close to the observed but can produce the MJO to a certain degree, the MJO physics suggested by their diagnostics may not be reliable. The practice of tuning a model to gain in MJO simulations at the cost of its background state moving away from observations can only produce misleading results and should not be encouraged [*Kim et al.*, 2011, 2014]. How close the background state of a model must be to observations for it to be a reliable tool for the MJO study is a subject for further investigation.

Acknowledgments
The test of our hypothesis (Figure 4) was suggested by two anonymous reviewers of a previous manuscript of this article. The authors thank the GASS-YoTC-MJO project for providing the model simulation data (https://earthsystemcog.org/projects/gass-yotc-mip/). This research was sponsored by the National Nature Science Foundation of China through grants 41575062 and 41520104008, Key Research Program of Frontier Sciences of CAS through grant QYZDB-SSW-DQC017, National Basic Research Program of China through grant 2015CB453200 (J.L.), by a NOAA grant NA13OAR4310161 through the Climate Variability and Prediction Program of the Climate Program Office (C.Z.), and by a NSF grant AGS-1543932 and NOAA/MAPP grant NA16OAR4310076 (S.W.). The PMEL contribution no. is 4625.

References

Ahn, M. S., D. Kim, K. R. Sperber, I. S. Kang, E. Maloney, D. Waliser, and H. Hendon (2017), MJO simulation in CMIP5 climate models: MJO skill metrics and process-oriented diagnosis, *Clim. Dyn.*, 1–23, doi:10.1007/s00382-017-3558-4.

Bechtold, P., M. Koehler, T. Jung, P. Doblas-Reyes, M. Leutbecher, M. Rodwell, and F. Vitart (2008), Advances in simulating atmospheric variability with the ECMWF model: From synoptic to decadal time scales, *Q. J. R. Meteorol. Soc.*, *134*, 1337–1351.

Benedict, J. J., E. D. Maloney, A. H. Sobel, D. M. Frierson, and L. J. Donner (2013), Tropical intraseasonal variability in version 3 of the GFDL atmosphere model, *J. Clim.*, *26*, 426–449.

Dee, D. P., et al. (2011), The ERA-Interim reanalysis: Configuration and performance of the data assimilation system, *Q. J. R. Meteorol. Soc.*, *137*, 553–597.

Fu, X., and B. Wang (2009), Critical roles of the stratiform rainfall in sustaining the Madden-Julian Oscillation: GCM experiments, *J. Clim.*, *22*, 3939–3959.

Gottschalck, J., P. E. Roundy, C. J. Schreck, A. Vintzileos, and C. D. Zhang (2013), Large-scale atmospheric and oceanic conditions during the 2011-12 DYNAMO field campaign, *Mon. Weather Rev.*, *141*, 4173–4196.

Hannah, W. M., and E. D. Maloney (2011), The role of moisture–convection feedbacks in simulating the Madden–Julian Oscillation, *J. Clim.*, *24*(11), 2754–2770.

Hannah, W. M., and E. D. Maloney (2014), The moist static energy budget in NCAR CAM5 hindcasts during DYNAMO, *J. Adv. Model. Earth Syst.*, *6*(2), 420–440.

Hayashi, Y., and D. G. Golder (1986), Tropical intraseasonal oscillations appearing in a GFDL general-circulation model and FGGE data.1. Phase propagation, *J. Atmos. Sci.*, *43*(24), 3058–3067.

Hendon, H. H., B. Liebmann, M. E. Newman, J. D. Glick, and J. E. Schemm (2000), Medium-range forecast errors associated with active episodes of the Madden-Julian Oscillation, *Mon. Weather Rev.*, *128*, 69–86.

Hirons, L. C., P. Inness, F. Vitart, and P. Bechtold (2013), Understanding advances in the simulation of intraseasonal variability in the ECMWF model. Part II: The application of process-based diagnostics, *Q. J. R. Meteorol. Soc.*, *139*(675), 1427–1444.

Huffman, G. J., D. T. Bolvin, E. J. Nelkin, D. B. Wolff, R. F. Adler, G. Gu, Y. Hong, K. P. Bowman, and E. F. Stocker (2007), The TRMM Multisatellite Precipitation Analysis (TMPA): Quasi-global, multiyear, combined-sensor precipitation estimates at fine scales, *J. Hydrometeorol.*, *8*(1), 38–55.

Hung, M. P., J. L. Lin, W. Q. Wang, D. Kim, T. Shinoda, and S. J. Weaver (2013), MJO and convectively coupled equatorial waves simulated by CMIP5 climate models, *J. Clim.*, *26*(17), 6185–6214, doi:10.1175/Jcli-D-12-00541.1.

Inness, P. M., and J. M. Slingo (2006), The interaction of the Madden-Julian Oscillation with the Maritime Continent in a GCM, *Q. J. Roy. Meteorol. Soc.*, *132*(618), 1645–1667.

Inness, P. M., J. M. Slingo, E. Guilyardi, and J. Cole (2003), Simulation of the Madden-Julian Oscillation in a coupled general circulation model. Part II: The role of the basic state, *J. Clim.*, *16*, 365–382.

Jiang, X., et al. (2015), Vertical structure and physical processes of the Madden-Julian oscillation: Exploring key model physics in climate simulations, *J. Geophys. Res. Atmos.*, *120*, 4718–4748, doi:10.1002/2014JD022375.

Kemball-Cook, S., B. Wang, and X. Fu (2002), Simulation of the intraseasonal oscillation in the ECHAM-4 model: The impact of coupling with an ocean model, *J. Atmos. Sci.*, *59*, 1433–1453.

Kiladis, G. N., J. Dias, K. H. Straub, M. C. Wheeler, S. N. Tulich, K. Kikuchi, K. M. Weickmann, and M. J. Ventrice (2014), A comparison of OLR and circulation-based indices for tracking the MJO, *Mon. Weather Rev.*, *142*, 1697–1715.

Kim, D., et al. (2009), Application of MJO simulation diagnostics to climate models, *J. Clim.*, *22*, 6413–6436.

Kim, D., A. H. Sobel, D. M. W. Frierson, E. D. Maloney, and I.-S. Kang (2011), A systematic relationship between intraseasonal variability and mean state bias in AGCM simulations, *J. Clim.*, *24*, 5506–5520.

Kim, D., et al. (2014), Process-oriented MJO simulation diagnostic: Moisture sensitivity of simulated convection, *J. Clim.*, *27*(14), 5379–5395, doi:10.1175/Jcli-D-13-00497.1.

Klingaman, N. P., X. Jiang, P. K. Xavier, J. Petch, D. Waliser, and S. J. Woolnough (2015), Vertical structure and physical processes of the Madden-Julian oscillation: Synthesis and summary, *J. Geophys. Res. Atmos.*, *120*, 4671–4689, doi:10.1002/2015JD023196.

Lafleur, D. M., B. S. Barrett, and G. R. Henderson (2015), Some climatological aspects of the Madden–Julian Oscillation (MJO), *J. Clim.*, *28*(15), 6039–6053.

Lau, N. C., and K. M. Lau (1986), The structure and propagation of intraseasonal oscillations appearing in a GFDL general-circulation model, *J. Atmos. Sci.*, *43*(19), 2023–2047.
Lau, W. K. M., and D. E. Waliser (2011), *Intraseasonal Variability of the Atmosphere–Ocean Climate System*, 2nd ed., p. 613, Springer, Heidelberg, Germany.
Lin, et al. (2006), Tropical intraseasonal variability in 14 IPCC AR4 climate models. Part I: Convective signals, *J. Clim.*, *16*, 2665–2690.
Ling, J., C. Y. Li, and X. L. Jia (2009), Impacts of cumulus momentum transport on MJO simulation, *Adv. Atmos. Sci.*, *26*(5), 864–876.
Ling, J., P. Bauer, P. Bechtold, A. Beljaars, R. Forbes, F. Vitart, M. Ulate, and C. Zhang (2014), Global versus local MJO forecast skill of the ECMWF model during DYNAMO, *Mon. Weather Rev.*, *142*(6), 2228–2247.
Ling, J., C. Li, T. Li, X. Jia, B. Khouider, E. Maloney, F. Vitart, Z. Xiao, and C. Zhang (2017), Challenges and opportunities in MJO studies, *Bull. Am. Meteorol. Soc.*, *98*, Es53-Es56.
Liu, P., Q. Zhang, C. Zhang, Y. Zhu, M. Khairoutdinov, H. M. Kim, C. Schumacher, and M. Zhang (2016), A revised real-time multivariate MJO index, *Mon. Weather Rev.*, *144*(2), 627–642.
Madden, R. A., and P. R. Julian (1971), Detection of a 40–50 day oscillation in zonal wind in tropical Pacific, *J. Atmos. Sci.*, *28*, 702–708.
Madden, R. A., and P. R. Julian (1972), Description of global-scale circulation cells in tropics with a 40–50 day period, *J. Atmos. Sci.*, *29*, 1109–1123.
Matthews, A. J. (2008), Primary and successive events in the Madden–Julian Oscillation, *Q. J. R. Meteorol. Soc.*, *134*, 439–453.
Miyakawa, T., Y. N. Takayabu, T. Nasuno, H. Miura, M. Satoh, and M. W. Moncrieff (2012), Convective momentum transport by rainbands within a Madden–Julian Oscillation in a global nonhydrostatic model with explicit deep convective processes. Part I: Methodology and general results, *J. Atmos. Sci.*, *69*, 1317–1338.
Mu, M., and G. Zhang (2008), Energetics of Madden Julian oscillations in the NCAR CAM3: A composite view, *J. Geophys. Res.*, *113*, D05108, doi:10.1029/2007JD008700.
Petch, J., D. Waliser, X. Jiang, P. Xavier, and S. Woolnough (2011), A global model inter-comparison of the physical processes associated with the MJO, GEWEX News, August.
Peters, K., T. Crueger, C. Jakob, and B. Mobis (2017), Improved MJO-simulation in ECHAM6.3 by coupling a stochastic multicloud model to the convection scheme, *J. Adv. Model. Earth Syst.*, *9*, 193–219, doi:10.1002/2016MS000809.
Salby, M. L., and H. H. Hendon (1994), Intraseasonal behavior of clouds, temperature, and winds in the tropics, *J. Atmos. Sci.*, *51*, 2207–2224.
Seo, K.-H., W. Wang, J. Gottschalck, Q. Zhang, J.-K. E. Schemm, W. R. Higgins, and A. Kumar (2009), Evaluation of MJO forecast skill from several statistical and dynamical forecast models, *J. Clim.*, *22*, 2372–2388.
Slingo, J. M., et al. (1996), Intraseasonal oscillations in 15 atmospheric general circulation models: Results from an AMIP diagnostic subproject, *Clim. Dyn.*, *12*, 325–357.
Sperber, K. R., J. M. Slingo, P. M. Inness, and W. K. M. Lau (1997), On the maintenance and initiation of the intraseasonal oscillation in the NCEP/NCAR reanalysis and in the GLA and UKMO AMIP simulations, *Clim. Dyn.*, *13*(11), 769–795.
Waliser, D. E., et al. (2003), AGCM simulations of intraseasonal variability associated with the Asian summer monsoon, *Clim. Dyn.*, *21*, 423–446.
Waliser, D., et al. (2009), MJO simulation diagnostics, *J. Clim.*, *22*(11), 3006–3030.
Wheeler, M. C., and H. H. Hendon (2004), An all-season real-time multivariate MJO index: Development of an index for monitoring and prediction, *Mon. Weather Rev.*, *132*(8), 1917–1932.
Wu, X., L. Deng, X. Song, G. Vettoretti, W. R. Peltier, and G. Zhang (2007), Impact of a modified convective scheme on the Madden-Julian Oscillation and El Niño-Southern Oscillation in a coupled climate model, *Geophys. Res. Lett.*, *34*, L16823, doi:10.1029/2007GL030637.
Yano, J.-I., R. Blender, C. Zhang, and K. Fraedrich (2004), 1/f noise and pulse-like events in the tropical atmospheric surface variabilities, *Q. J. R. Meteorol. Soc.*, *130*, 1697–1721.
Zhang, C. (2013), Madden-Julian Oscillation: Bridging weather and climate, *Bull. Am. Meteorol. Soc.*, *94*(12), 1849–1870.
Zhang, C., and H. H. Hendon (1997), Propagating and stationary components of the intraseasonal oscillation in tropical convection, *J. Atmos. Sci.*, *54*, 753–767.
Zhang, C., and J. Ling (2017), Barrier effect of the indo-pacific maritime continent on the MJO: Perspectives from tracking MJO precipitation, *J. Clim.*, *30*, 3439–3459, doi:10.1175/JCLI-D-16-0614.1.
Zhang, C., M. Dong, S. Gualdi, H. H. Hendon, E. D. Maloney, A. Marshall, K. R. Sperber, and W. Wang (2006), Simulations of the Madden-Julian Oscillation by four pairs of coupled and uncoupled global models, *Clim. Dyn.*, *27*, 573–592.
Zhang, G. J., and M. Mu (2005), Simulation of the Madden–Julian Oscillation in the NCAR CCM3 using a revised Zhang–McFarlane convection parameterization scheme, *J. Clim.*, *18*, 4046–4064.
Zhou, L., R. B. Neale, M. Jochum, and R. Murtugudde (2012), Improved Madden-Julian oscillations with improved physics: The impact of modified convection parameterizations, *J. Clim.*, *25*, 1116–1136.